Circulating Fluid-Bed Technology for Advanced Power Systems

Lawrence J. Shadle[*], J. Christopher Ludlow[*], Joseph S. Mei[*], and Christopher Guenther[+]
[*]National Energy Technology Laboratory
[+]Fluent Inc.
U. S. Department of Energy
Morgantown, West Virginia 26507-0880

Introduction

Circulating fluid bed technology offers the advantages of a plug flow, yet well-mixed, and high throughput reactor for power plant applications. The ability to effectively scale these systems in size, geometry, and operating conditions is limited because of the extensive deviation from ideal dilute gas-solids flow behavior (Monazam et al., 2001; Li, 1994). Two fluid computations show promise of accurately simulating the hydrodynamics in the riser circulating fluid bed; however, validation tests for large vessels with materials of interest to the power industry are lacking (Guenther et al., 2002). There is little available data in reactors large enough so that geometry (i.e. entrance, exit, and wall) effects do not dominate the hydrodynamics, yet with sufficiently large particle sizes to allow sufficiently large grid sizes to allow accurate and timely hydrodynamic simulations. To meet this need experimental tests were undertaken with relatively large particles of narrow size distribution in a large enough unit to reduce the contributions of wall effects and light enough to avoid geometry effects. While computational fluid dynamic calculations are capable of generating detailed velocity and density profiles, it is believed that the validation and model development begins with the ability to simulate the global flow regime transitions. The purpose of this research is to generate well-defined test data for model validation and to identify and measure critical parameters needed for these simulations.

Experimental Methods

The test unit configuration is shown in Figure 1. The solids enter the riser from a side port 0.23-m in diameter and 0.27-m above the gas distributor. Solids exit the riser through a 0.20-m port at 90^{o} about 1.2-m below the top of the riser at a point 15.45-m above the solids entry location (centerline to centerline). Riser velocities were corrected for temperature and pressure as measured at the base of the riser. The air's relative humidity was maintained between 40 and 60% to minimize effects of static charge building up on the solids. Pressure drop resulting solely from gas flow was neglected. Twenty incremental differential pressures were measured across the length of the riser using transmitters calibrated within 0.1 % of full-scale or about 2 Pa/m. The primary response measurement was the overall riser pressure differential and it was calibrated within 0.45 Pa/m. Mass circulation rate was continuously recorded by measuring the rotational speed of a twisted spiral vane located in the packed region of the standpipe bed (Ludlow et al., 2002). This volumetric flow measurement was converted to a mass flux using the measured packed bed density presented in Table 1 and assuming that the packed bed void fraction at the point of measurement was constant.

The operator varied operating conditions by adjusting the riser flow or solids circulating rate while maintaining constant system outlet pressure at 0 psig. The solids circulation was varied by controlling the aeration at the base of the standpipe and by adjusting the total system inventory to increase the standpipe bed height. Steady state conditions were defined as holding a constant set of flow conditions and maintaining a constant response in the pressure differentials over a five-minute period.

Table 1. Bed material properties.

Cork characteristics:		
ρ_s	kg/m^3	189
ρ_b	kg/m^3	95
d_{sv}	μm	812
U_t	m/s	0.86
U_{mf}	m/s	0.07
ε_{mf}		0.49
ϕ		0.84

Fluidization bed material properties are presented in Table 1. A relatively light bed material was selected to generate data relevant for advanced high-pressure coal conversion processes. According to a Buckingham-Pi analysis of the riser in a CFB the ratio of gas: solids density is critical factor important in scaling from a model, such as these cold flow tests, to a prototype application, such as a high pressure and high temperature transport reactor (Ghordzoe et al., 2001). Cork offers an excellent bed material which when tested at ambient conditions in air yields a similar density ratio to that of coal processed at 10-20 atmospheres and 1000 C. The particle density was measured using water displacement taking care to wet the surface completely. The cork surface is sufficiently hydrophobic to avoid filling any porosity with water. The particle size was measured using standard sieve analysis. The size distribution is displayed in Figure 2. The minimum fluidization velocity was measured in the loopseal by closing the slide gate valve in the standpipe and increasing the gas velocity while measuring an incremental pressure drop across the loopseal. In addition, the shape factor for this natural wood material is expected to be comparable to that of coal that was derived from woody tissues and retains much of its morphology. The sphericity was estimated fitting the Ergun equation to the pressure drop - velocity profile taken prior to fluidization. The terminal velocity was calculated from drag laws using the measured solids density and particle size, and sphericity.

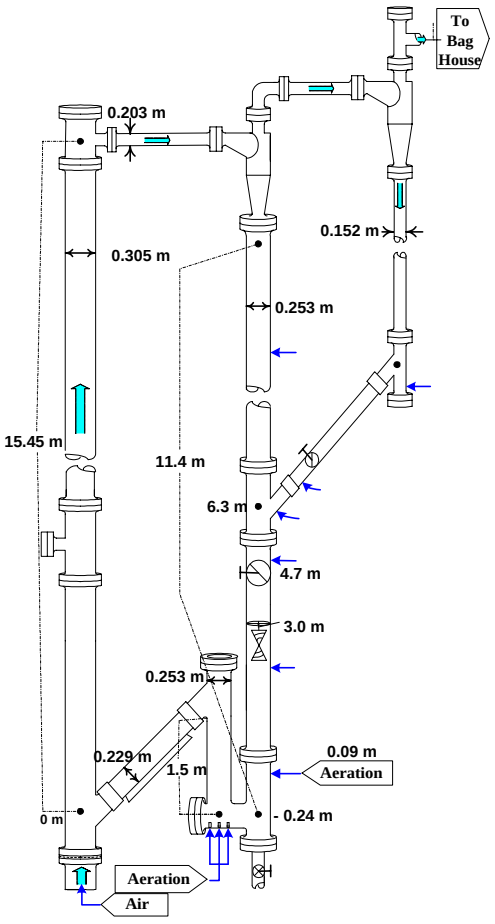

Figure 1. Schematic of CFB test unit indicating gas-solids separation and aeration location.

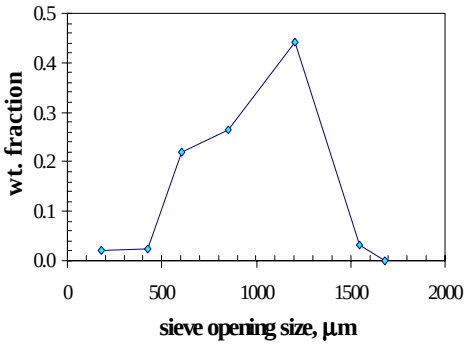

Figure 2. Typical size distribution of cork bed material.

Experimental Results & Discussion

In order to identify the operating conditions several tests and data analyses were performed. The voidage profiles were characterized as a function of operating conditions. For a given gas velocity the solids circulation rate gradually increased, the flow regime changed from dilute-phase flow to fast fluidization, and to dense phase flow. As displayed in Figure 3A, the voidage profiles changed from C-shaped to S-shaped up to homogenous or uniform axial profiles (Figure 3A). When operating with the riser in the S-shaped profile the voidage in the bottom dense

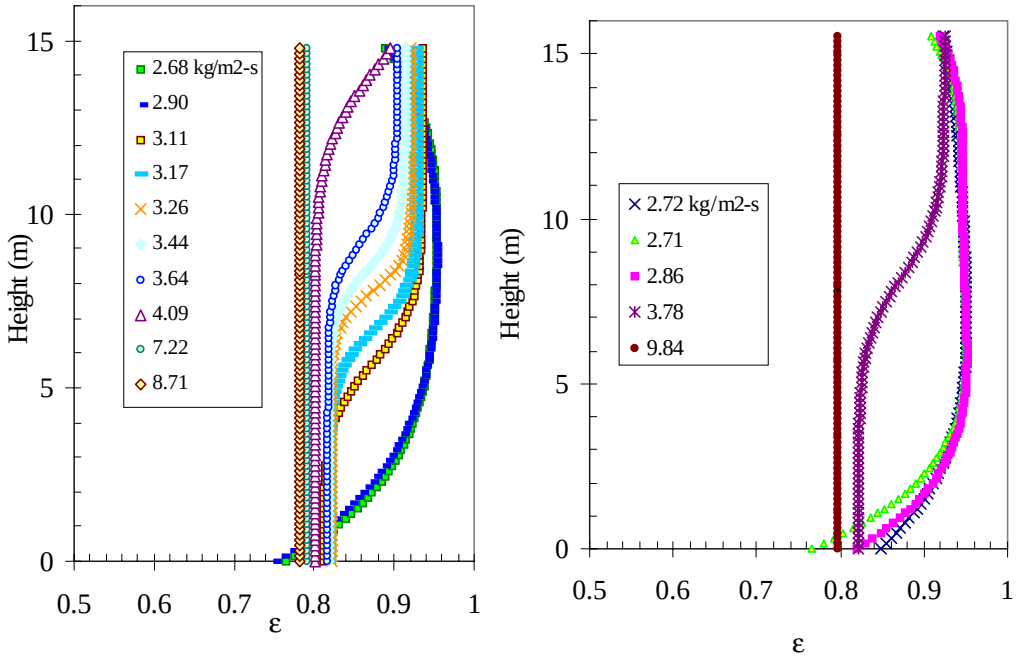

A) B)

Figure 3. Voidage profiles as a function of mass flux for two gas velocities: A) 3.2, and B) 3.4 m/s.

region of the riser does not change appreciably with changes in solids flow rate as long as the riser velocity is constant as reported by King (1989) and Li (1994). Once the S-shape profile was fully developed with a constant solids fraction at the bottom and top, gradually increasing the circulation rate resulted in an increased dense bed height. In other words the inflection point between the dense and dilute beds regions increased, up to a circulation rate characterized by a riser that was fully filled with dense bed.

At a higher gas velocity (Figure 3B) the range of mass fluxes that produced S-shaped profiles decreased. The transition from dilute to fully filled dense bed was narrower. The height of the acceleration zone at the bottom and length of the dense bed at the top

depends upon the particle's terminal velocity and the gas velocity. At lower velocity the acceleration zone was pronounced - extending over 5 m up the length of the riser. As might be expected, this acceleration zone was shorter at the higher gas velocity. When sufficient mass flux was introduced to the riser the acceleration zone disappeared or rather was converted to a uniformly dense bed region over a considerable length at the bottom of the riser.

At the low flow case the solids fraction near the exit nearly doubled compared to the solids fraction in the middle of the riser. This increased solid loading near the exit occurred only when operating below the fully developed S-shaped profile. But in the high flow case the solids fraction at the outlet was only about 25% greater than that in the middle of the riser. The exit effect was less prominent for the higher gas velocity. This trend tended to reverse itself when operating well above the terminal velocity of solids.

The transition from a dilute to a dense bed was measured by halting the solids flow when the riser was in the fast fluidized regime and contained at least some dense bed character (Monazam et al., 2001). The transient test data was analyzed by taking the first derivative of the riser pressure drop with respect to time. The associated mass flux value at time=0 is referred to as the Saturation Carrying Capacity (SCC) because this is the most solids that a given velocity of gas can carry within the Fluid-Dominated (FD) regime (Li, 1994) without collapsing and forming a denser bed and entering the Particle-Fluid Compromising (PFC) regime (Li, 1994).

Table 2. Saturated Carrying Capacity (SCC) as measured from solids cut-off experiments at various Steady State (SS) test periods.

		riser at SS	SS	SCC
test no.	U_g(m/s)	$\Delta P/\Delta L$ (Pa/m)	G_s (kg/m^2-s)	G_s (kg/m^2-s)
ck48	2.81	217	2.50	1.96
ck71	2.94	226	2.44	2.20
ck138	3.09	232	3.45	3.07
ck128	3.24	232	3.78	3.61
ck129	3.39	207	4.82	4.65

A comparison between the SCC and the steady-state mass flux revealed close agreement (Table 2); with the SCC always slightly lower than the steady-state solids flux. This is because the SCC represents the upper limit for the FD regime and the lower boundary for the PFC regime. The dependence of the SCC with gas velocity is presented graphically in Figure 4. There was only a relatively small range of conditions that produced an S-shape riser voidage profile. Above 3.4 m/s the cork did not produce a discernible S-shaped riser profile. We speculate that this may be a result of the corks narrow-size distribution or relatively large cork particles compared to PVC and coke materials studied previously. The transport velocity is thought to be above this point where no dense bed or S-shaped voidage profile can be formed. However, an accurate observation of the transport velocity is difficult experimentally.

The correlation developed by Monazam et al. (2001) was applied to this cork data and is also presented in Figure 4. The correlation was found to be quite sensitive to the

cork terminal velocity. It is apparent that simple calculation of the terminal velocity based on difficult measurement of particle properties can lead to large inaccuracies. In addition, the tendency for particles to cluster and the potential segregation of particles in the riser lead to further ambiguities in the critical particle properties required normalize and generalize the hydrodynamic relationships.

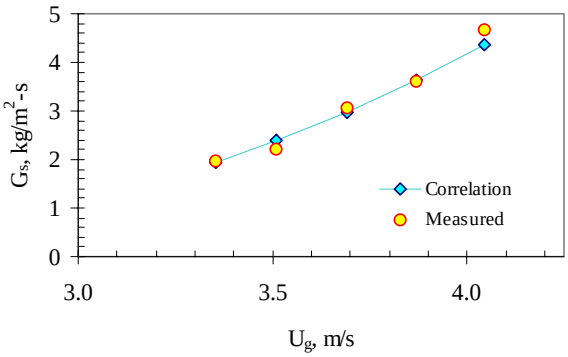

Figure 4. Saturated carrying capacity as measured for cork using solids cut-off tests compared to estimates from SCC correlation (Monazam, 2001).

As indicated above, the void fraction in the dense section at the base of the riser when operating in the S-shaped profile is a function of gas velocity. Thus, the maximum pressure that can be generated in a riser of fixed height is also a function of U_g when the riser is completely filled with a dense bed. Experimentally this maximum pressure drop can be calculated knowing the solids fraction in the dense bed of the riser in the S-shaped or dense regime using the following equation:

$$\Delta P_{r,max} = \rho_s \cdot (1-\varepsilon_{dense}) \cdot H_{riser}$$

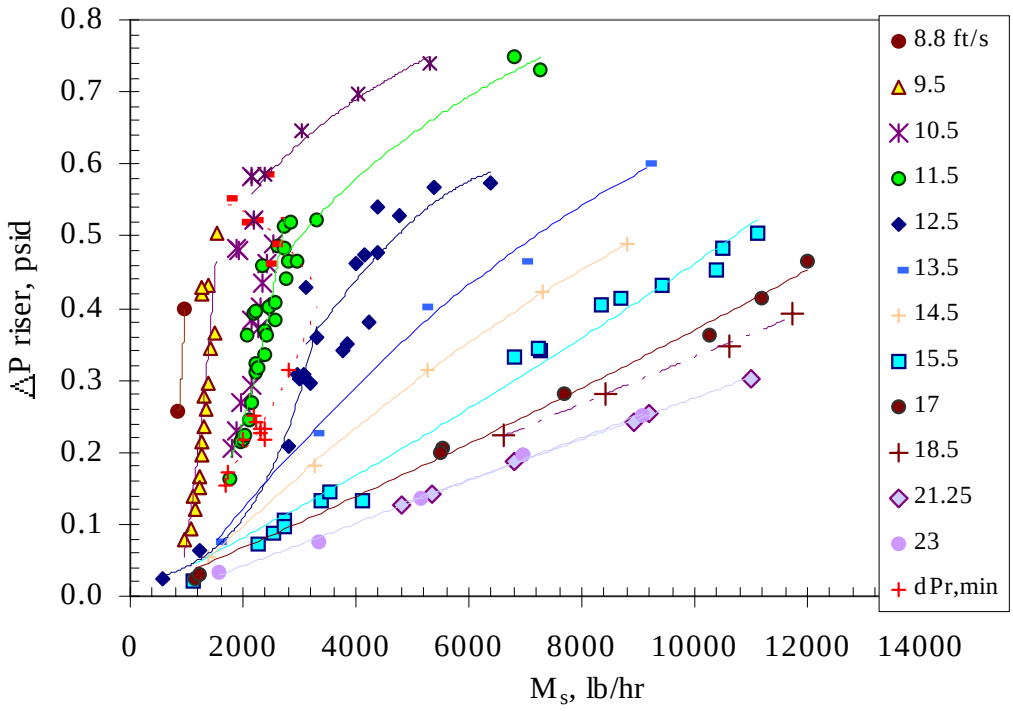

Figure 5. The variation in ΔP/ΔL with solids flux and gas velocity over the entire riser.

As expected the maximum riser ΔP in the riser (i.e. $\Delta P_{r,max}$) was always greater than that of the steady state and this value decreased slightly with increasing gas velocity. The transport velocity can be thought of as the U_g where the riser ΔP at SCC is equal to $\Delta P_{r,max}$.

In Figure 5 the riser operating regime is mapped using the riser inventory as the dependent variable over a range gas and solids velocities. The solids flux is presented as the independent parameter using a series of constant riser gas velocities and the response variable is measured by the riser ΔP over the length of the riser. The red lines depict the regime transitions. The red line with negative slope at higher ΔPs demarcates the transition from fast fluidization regime (between a partially filled riser (below the line)) to dense phase flow regime (one that is completely filled with a more dense bed (above the line)). The red line at lower ΔPs with the positive slope marks the SCC transition. This is the transition from a dilute-phase flow regime (below the line) to the fast fluidization regime with a developing dense bed at the bottom or the riser (above the line)).

Computational Fluid Dynamic Modeling Results and Discussion

The computational fluid dynamic simulations were conducted using the MFIX Code developed here at NETL. MFIX simulations were setup using Cartesian co-ordinates. A two-dimensional (2D) axisymmetric simulation would appear to be the natural choice for approximating the cylindrical riser section; however, non-physical clusters form at the centerline in such simulations. Hence, we chose a 2D Cartesian grid in this preliminary investigation to compare high order limiters. The computational grid consisted of 30 cells in the x-direction and 860 cells in the y-direction and no-slip boundary conditions were used for both phases. Three dimensional (3D) cylindrical simulations were also conducted using 1 cm size grids in the radial and axial directions, and 6 uniform wedge shaped slices in the θ - direction. Initially, the riser was void of any solids (empty) corresponding to the experimental conditions at start-up. The voidage and solids velocity at the side inlet and the gas velocity at the base of the riser were held constant during each simulation. Also, additional air (move air) was specified with the solids to account for the fluidizing air used in the loopseal and at the base of the standpipe during operation.

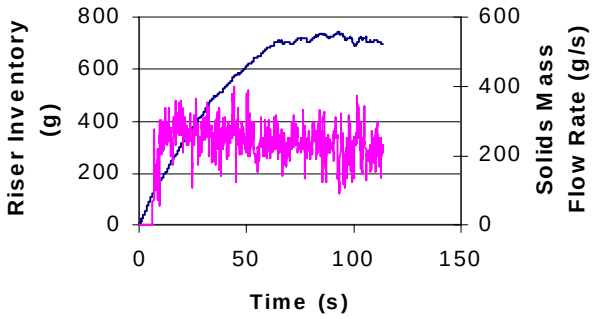

Figure 6. MFIX simulation of CFB Riser showing approach of inventory (—) and solids flow rate (—) to steady-state condition.

Each simulation was run until 10-15 seconds of data at steady-state conditions was collected. In this investigation steady state was determined when the total solids inventory

in the riser did not show any large fluctuations over time (Figure 6). This criteria for steady state required longer run times than using solids circulation rate as a criteria. In fact, solids circulation rates reached steady-state conditions well before the solids inventory in the riser did and should not be used to determine steady-state conditions. Typically, simulations required 80-120 seconds of data to be collected using only the final 10-15 seconds in our analysis. Simulations were conducted on high-end dual processor PC's and run times were generally on the order of three-four weeks.

In the simulations previously reported in the literature, the calculated pressure drop is usually less than the experimental value, and to match the experimental data, parameters such as the solids viscosity or the drag are adjusted (see for example, O'Brien and Syamlal 1993). The studies previously reported in the literature are for smaller (100 μm) diameter particles. The simulation of an industrial-scale CFB using these small particles with sufficiently small grid is computationally prohibitively expensive. This difficulty has lead to the need for developing subgrid scale models (Agrawal et al. 2001) that will allow the use of coarse grids. For the nearly 1000 μm diameter particles used in this study, it appears that a grid resolution of about ten times the particle-diameter is sufficient to calculate pressure drop values that match experimental data, without adjusting any physical parameters.

Numerical dispersion was found to result in inaccurate simulations. Varying the numerical discretization methods and the use of higher order limiters tested this. In Figure 7 the simulated riser pressure profiles calculated using various higher order convergence algorithms are compared with the experimental data. Both the 2D and 3D simulations were tested. Both 2D and 3D had good agreement with experimental pressure data, and predicted clustering and core annular structure. Higher order numerical algorithms reduced the effects of numerical dispersion.

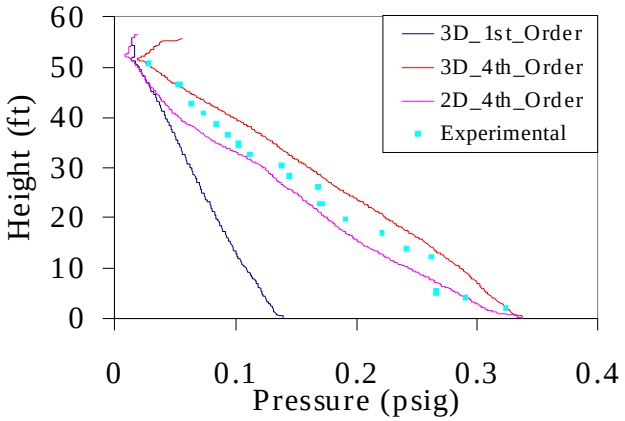

Figure 7. Comparison of the riser profiles predicted with MFIX using different numerical algorithms.

The 2D simulations, however, exaggerated the solids recirculation near the entrance and exit of the riser. This is due to the limited spatial options available in 2D simulations for flow to bypass obstructions near the ends of the riser such as a cluster of solids. In these simulations large solids fluxes were observed near the walls due to the development of internal solids circulation patterns with solids traveling up to the exit on the side of the wall and down the opposite wall. Likewise the pressure drop at the entrance was under predicted because the gas flow did not have anywhere to travel but through the solids inlet stream. In addition the solids in the riser were not readily elutriated or transported out of the riser as compared to the experimental measurements,

even when the solids inlet flow was dropped to zero. The strong recirculation patterns contributed to excessively long riser emptying times for these shutdown runs.

Three dimensional (3D) simulations improved the exit and entrance effects by reducing the strong recirculation patterns compared to the 2D simulations. In addition the solids flux near the walls were markedly lower. The 3D simulations with 1 cm radial grid spacing achieved acceptable run times ~ 3weeks using 2 and 4 node Beowulf clusters. However, wide variation in radial profile were predicted (Figure 8). We have not yet obtained the experimental data to confirm these predictions. A set of consistent test data on both solids loading and velocity are needed to evaluate these simulations and explore the effects of numerical discretization methods and higher order limiters in the radial direction. Boundary conditions at the wall and particle properties both need to be better defined.

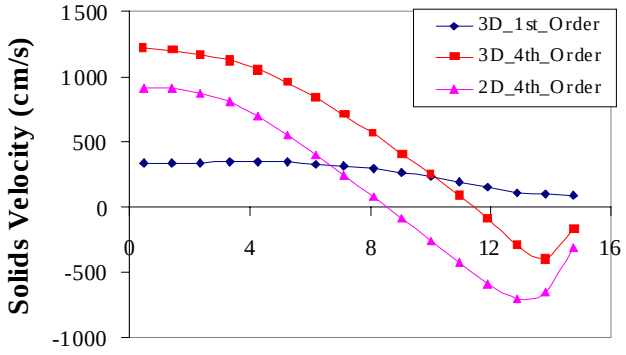

Figure 8. Comparison of the radial solids velocity profiles in the riser predicted with MFIX using different numerical discretization methods.

Conclusions

A Cold Flow Circulating Fluid Bed (CFCFB) having diameter of 0.3 m-ID and 15 m-high riser, was operated under ambient conditions and at different fluidization flow regimes. Identification of fluidization flow regimes and their boundaries is critical to CFB operation and performance. In this work the flow regimes were studied from homogeneous a dilute-phase flow regime to a dense-phase fluidization flow regime. Operating flow regime was evaluated and axial voidage profiles along the riser for different flow regimes were characterized as a function of gas velocities and mass fluxes. Saturated carrying capacities were determined as a function of riser velocity using the solids cut off method. Coarse cork particles were employed in the experiments to facilitate computational fluid dynamic model validation.

Two and three dimensional (2D and 3D) simulations of the riser section of the CFB were performed using the MFIX code over a range of solids circulation rates and riser gas velocities for cork with the CFCFB configuration. Riser inventory was shown to be the appropriate quantity for determining when steady-state conditions have been reached and field variables should be time-averaged. Grid size independence was established. This investigation also found inconsistencies in the prediction of riser inventories when using different high order limiters. Pressure profiles along the height of the riser were matched well for both the 2D and 3D simulations. The 2D simulations displayed exaggerated entrance and exit effects. Also, substantial differences were observed in the radial profiles (solids velocities and concentration), especially near the

vessel wall when testing various numerical discretization methods. Sufficient data is unavailable to adequately verify the simulations of the radial solids and velocities distributions.

Notation

$d_{p,50}$	mean particle size at 50 at percent (μm)	SCC	saturated carrying capacity (kg/m^2s)
d_{sv}	Sauter mean particle size (μm)	U_g	superficial gas velocity (m/s)
D	riser diameter (m)	U_{mf}	minimum fluidization velocity (m/s)
G_s	solids flux (kg/m^2s)	U_t	particle terminal velocity (m/s)
H	riser height (m)		
P	pressure (kPa)		

Greek letters

ΔP_r	pressure drop across the riser (kPa)	ρ_s	solid particle density (g/cc)
$\Delta P/\Delta L$	pressure drop per unit length (Pa/m)	ρ_b	bulk density (g/cc)
ε	voidage	ϕ	particle sphericity
ε_a	limiting voidage of the dense phase		
ε_{mf}	voidage at minimum fluidization (m/s)		

Acknowledgments

The authors would like to acknowledge the Gasification Technologies, Combustion Systems, and Advanced Power Research Product lines of the U.S. Department of Energy for funding various aspects of this research. The authors also would like to acknowledge Esmail R. Monazam of REM Engineering and Jim Devault and Larry O. Lawson of the Department of Energy for their contributions in collecting test data and conducting data analysis used in this report.

References

Agrawal, K., P.N. Loezos, M. Syamlal, and S. Sundaresan, "The role of meso-scale structures in rapid gas-solids flows", accepted for publication in *the Journal of Fluid Mechanics*, 2001.

Ghordzoe, E, P. Smith, P. Vimalchand, G. Lui, and J. Longanbach, " Initial operations of the PSDF Transport Gasifier*", Proceedings of the 16th International Conference on Fluidized Bed Combustion*, FBC01-0065, Reno, Nevada, 2001.

Guenther, C., M. Syamlal, L.J. Shadle, C. Ludlow, **"**A Numerical Investigation of an Industrial Scale Gas-Solids CFB", *7th International Circulating Fluid Bed Conference*, in press, Niagara Falls, Canada, 2002.

King, D.F., "Estimation of Dense Bed Voidage in Fast and Slow Fluidized Beds of FCC Catalysts", in *Fluidization VI*, ed. by J.R. Grace, L.W. Shemilt, and M.A. Bergougnou, New York, 1(1989)

Li, Jinghai, "Modeling" in *Advances in Chemical Engineering, Volume 20, Fast Fluidization*; ed. by M. Kwauk, Academic Press, Inc., San Diego, 148(1994).

Ludlow, C., L. O. Lawson, and L. J. Shadle, “Development of a Spiral Device for Measuring the Solids Flow in a Standpipe”, *7th International Circulating Fluid Bed Conference*, in press, Niagara Falls, Canada, 2002.

Monazam, R.E.; L.J. Shadle; and L.O. Lawson, “A Transient Method for Determination of Saturation Carrying Capacity”, *Powder Technology*, **121**, 205-212 (2001).

O’Brien, T.J. and M. Syamlal, ”Particle Cluster Effects in the Numerical Simulation of a Circulating Fluidized Bed,” in Circulating Fluidized Bed Technology IV, Ed. A. Avidan, *Proceedings of the Fourth International Conference on Circulating Fluidized Beds*, Somerset, PA, August 1-5, 1993.